# Reducing Air Pollutants in A Kitchen Environment

Y.X. Kong, Haslinda M. Kamar*, Nazri Kamsah

Faculty of Engineering
Universiti Teknologi Malaysia
81310 UTM Johor Bahru
Johor, Malaysia

## ABSTRACT

*Excessive $CO_2$ from a gas stove could cause sick building syndrome. Therefore, it is essential to investigate the distribution and concentration of the $CO_2$ in a kitchen area. The primary goal of this research is to reduce the pollutants in the kitchen environment by examining the effects of airflow velocity and the use of the range hood on the concentration of $CO_2$ and CO gases. A computational fluid dynamics (CFD) method was employed and a grid independent test (GIT) that is providing an accurate solution was used to determine the number of elements. The model was then validated by comparing its result with the experimental data obtained from the literature. The shear stress transport (SST) k-φ model was chosen in the study and it was then simulated considering four cases with different conditions. The best result was then compared with the worst. By changing the conditions of a window, the pollution level can be reduced by 9.35% which was relatively ineffective compared to increasing the velocity of the range hood. By changing the hood's velocity from 1.88 m/s to 5.22 m/s, the concentration of $CO_2$ can be reduced by 17.09%. Moreover, the installation of a range hood can help the room decreased the $CO_2$ level by 57.33% if compared to the case without the hood. Hence, it can be concluded that the velocity of the range hood is a parameter that is more significant than the conditions of the window. Besides, by changing the velocity of the range hood from the lowest to highest speed, the average concentration of CO in the cooking area has been reduced by 4.56%, while the level of CO in the adjacent room reduced by 8.84%.*

**Keywords**: *Range hood, velocity of outlet, CO, $CO_2$, pollutants, kitchen*

## 1.0 INTRODUCTION

The kitchen is always a tough and high-stress environment to work in. Not to mention the temperature in the kitchen was relatively high compared to the other working environments and yet occupant will always get surrounded by cooking oil fume. If the temperature in the space increases by 5.5°C above the comfort level, the productivity may drop as much as 30% [1]. All ideas or discussions here can be applied to both cases, either in a commercial kitchen or residential kitchen. Low productivity indicated that there are lots of time will be wasted, and it is unnecessary and can be avoided by having a good ventilation system in the kitchen [2, 3]. Besides the productivity losses, a high temperature in a commercial kitchen also contributed to a very high turnover rate, and eventually, profit loss for the restaurant operator will be affected.

*Corresponding email: haslinda@utm.my

Other than the productivity, a bad ventilation system in the kitchen may also cause a person to get sick building syndrome. Sick building syndrome (SBS) is used to describe situations in which building occupant experienced acute health and comfort effects. A study shows the $CO_2$ concentration, indoor temperature, and relative humidity are the factors which contribute to the symptoms of SBS.

A study states that there was a positive correlation between the cooking frequency and the lung cancer [4]. There is an average of 1650 to 1750 women dying of lung cancer per year in Taiwan, which constitutes one-sixth of all female cancer patients [4]. Since most people spend 90% of the time indoors, the indoor environment had a significant influence on human health [5, 6]. Regarding the indoor particle sources, ultra-fine particles (UFP) which sized from 0.1 to 10 µm can be generated within the area where smoking and cooking take place, which happened to be the two most significant contributions of the concentration of indoor space [5]. Combustion was the primary source of carcinogenic polycyclic aromatic hydrocarbons (PAHs). PAHs produced by cooking contains both the low molecular weight gaseous PAHs and the particulate-phase PAHs [7]. The latter contributed more severe health threat than the benzo[a]pyrene when the concentration of the particulate-phase PAHs was more than 95%. Small particulate particles are more likely to cause cardiovascular disease because they will easily transport through the blood stream [7]. Hence, a study must be conducted to find an optimal method of pollutants' control in the kitchen area.

## 2.0 MATERIALS AND METHOD

### 2.1 Geometry

SolidWorks software was used to develop a computational domain of a residential kitchen. The kitchen model is shown in Figure 1. The kitchen area was extruded to 2.4 m height with a wall thickness of 0.15 m. The dimension of the floor area is given in centimeters as shown in Figure 2.

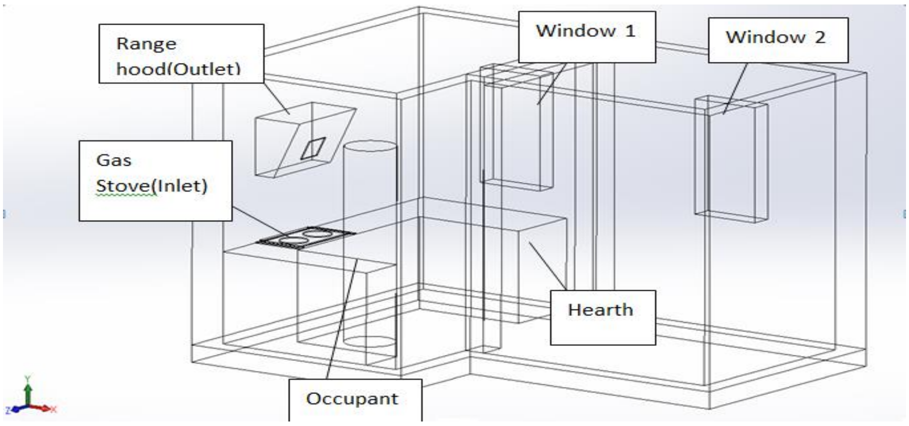


**Figure 1**: CFD model of a kitchen

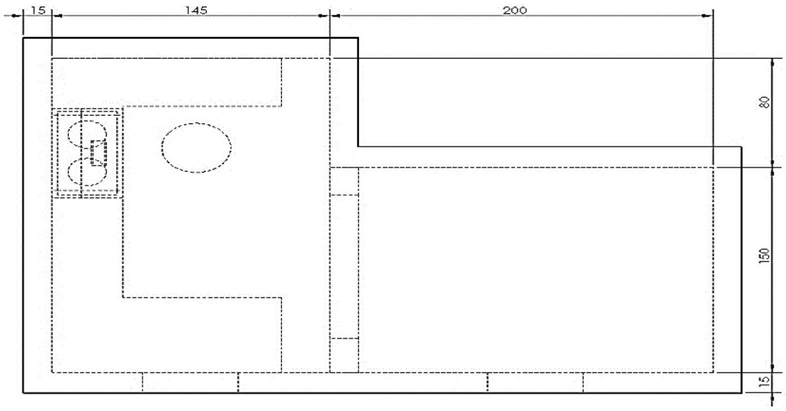


**Figure 2:** Top view of the kitchen area

The dimensions of the kitchen model are based on a kitchen model adopted from work done by Zhou *et al*. [7]. The kitchen consists of a hearth that covered most of the kitchen area, and there are two gas stoves above a fireplace. The occupant shape is simplified as a cylinder with a height of 1.6 m and 0.18 m radius. The hearth's height is 0.8 m while the outlet of range hood is 0.18 m × 0.18 m. A radius of the outlet gas stove is 0.1 m. For both windows, the height and length are 1 m and 0.5 m, respectively.

## 2.2 Meshing

The model was then exported to the CFD software for the meshing process [8, 9]. The process was done to subdivide the space in the domain into grid cells. A smaller size of grid cells gives a more substantial number of elements generated by meshing, and a more accurate simulation result [10].

Five meshing with a different number of elements were generated based on the CFD model of the residential kitchen area in conducting verification and validation. The concentration of $CO_2$ was chosen for the parameter to carry out the grid independent test (GIT). The first mesh has 81411 elements, the second mesh has 92937 elements, the third mesh has 116877 elements, the fourth mesh has 333927 elements, and the fifth mesh has 2465436 elements. The same type of meshing was used, but it varies with the minimum proximity size whereby the fine cells generated around the high-gradient-region become even finer. The concentration of $CO_2$ has been taken as the parameter to carry out the GIT. The average concentration of $CO_2$ along Line 1 as shown in Figure 3 is taken and compared for each number of elements. For Line 1, it is formed by two points with coordinates (-3.25, -1.5, -0.06) and (-3.25, -1.1, -0.06). The average concentration of $CO_2$ for each number of elements is then tabulated in Table 1.

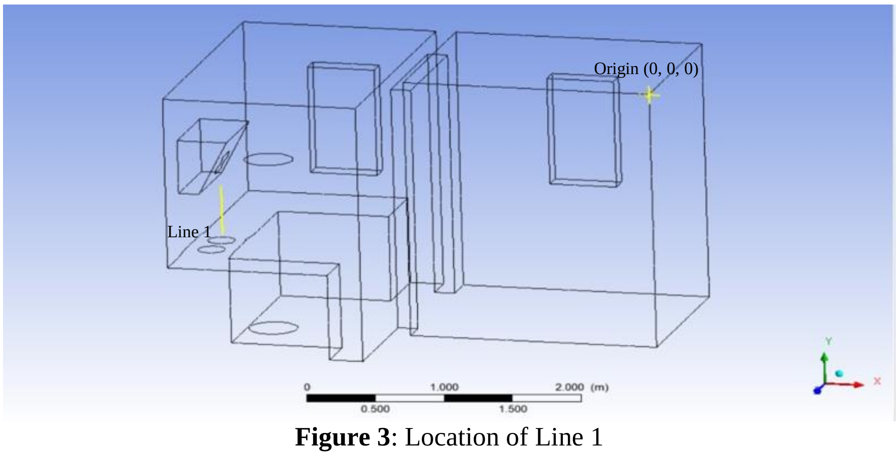


**Figure 3**: Location of Line 1

**Table 1:** Average concentration of $CO_2$ along Line 1

| Number of elements | Average concentration of $CO_2$ along Line 1 (%) |
|---|---|
| 81411 | 1.84 |
| 92937 | 1.55 |
| 116877 | 1.86 |
| 333927 | 2.01 |
| 2465436 | 1.94 |

The GIT graphs show the parameters of a concentration of $CO_2$ are independent of 300k of elements onwards. Even though the number of elements is further increased to 2.4 million elements, the results have only insignificant change. Moreover, these data plotted are extracted from CFD-post processing with the accuracy up to six significant figures. Therefore, it can be concluded that 333927 elements are the optimum number of elements whereby the result does not change significantly even though the number of elements is further increased.

## 2.3 General Setup

For the average concentration of $CO_2$ and CO along the cooking area and adjacent room, it was determined via exporting the data of Lines 2 and 3 as shown in Figure 3 to Microsoft Excel software.

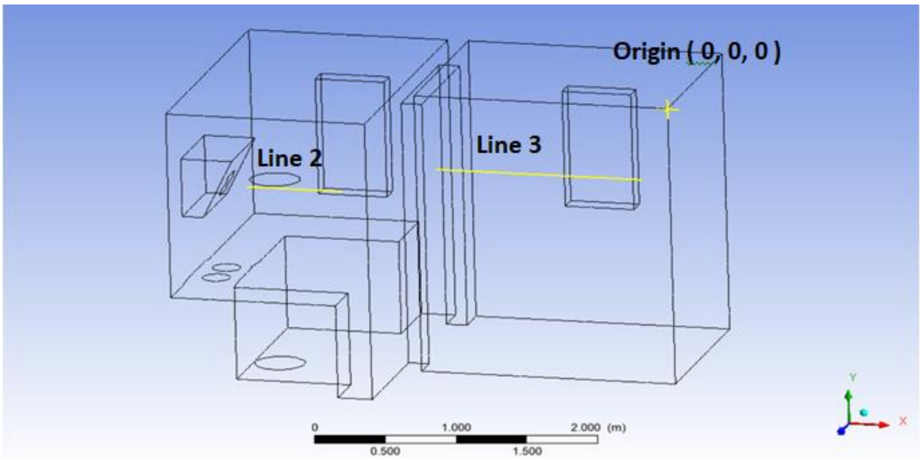


**Figure 3:** Line 2 and Line 3

For Line 2, it is formed by two points with coordinates (-3.1, -0.9, 0.05) and (-2.4, -0.9, 0.05). For Line 3, it is formed by two points with coordinates (-0.4, -0.88, -0.755) and (-1.9, -0.88, -0.755). Both lines lie on the plane 1.5 m above the ground. It is because the occupant's height is 1.6 m and 1.5 m are the breathing zone for the occupant which may endanger an occupant's health if the concentration of the pollutant in this area is critical. The average concentration of $CO_2$ along Line 2 was collected which is along the cooking area at the plane, breathing zone. The data was then compared to the experimental data obtained from the literature. Validation was carried out for four models which are one equation model, the standard k-$\varepsilon$ model, re-normalization group (RNG) $k$-$\varepsilon$ model and *Menter's* shear stress transport (SST) $k$-$\varphi$ [11, 12]. All the models were run for the baseline model. The model with the closest result compares to the experimental data was adopted [13]. The data collected along Line 2 is then tabulated in Table 2. For the experimental data, the average concentration of $CO_2$ along Line 2 is 0.878%.

**Table 2:** $CO_2$ concentrations for four models

| Model | Average concentration $CO_2$ (%) | Percentage of error (%) |
|---|---|---|
| One equation | 0.782 | 10.93 |
| Standard $k$-$\varepsilon$ | 1.15 | 30.97 |
| RNG $k$-$\varepsilon$ | 1.1 | 25.28 |
| SST $k$-$\omega$ | 0.861 | 1.25 |

The SST $k$-$\omega$ turbulent model was applied in this study for all the cases since its result is the closest to experimental data. The range hood, gas stoves, occupant, hearth and air curtains were set as solid whereas fluid occupied the remaining volume in the kitchen. The boundary conditions were determined and set to carry out further simulation. The boundary conditions are summarized in Table 3. From the study, the mole fraction of the products comes from the liquefied petroleum gas combustion and that the best heat source temperature should be 1240k. In this study, according to the characteristics of flame, the heat source temperature was set to be 1400 K [7].

**Table 3:** Boundary conditions at different locations

| Location | Type | Boundary condition | |
|---|---|---|---|
| | | Air | $CO_2$ and CO |
| Gas Stove | Velocity inlet | Velocity = 0.6 m/s<br>Temperature =1400 K | Velocity = 0.6 m/s<br>Temperature = 320 K |
| Window | Pressure Outlet | Pressure = 1 atm | |
| Range Hood | Velocity Outlet | Velocity = 1.88 m/s | |
| Hearth | Wall | Momentum: Stationary wall no slip | |
| Occupant | Wall | Momentum: Stationary wall no slip<br>Heat generation rate: 104.67 W | |

### 2.4 Solver and Solution Method

A simple scheme was used for the pressure-velocity coupling in the calculation. For spatial discretization, the second-order upwind scheme was used in solving differential derivatives for both momentum and energy. The reason is that the second-order upwind scheme is more accurate than the first order upwind scheme. Residual plays a role in determining how accurate the data are. The residual monitor can be said as the maximum allowable error of the residual for continuity, $x$-velocity, $y$-velocity, $z$-velocity, $k$-$\varepsilon$, and energy. According to the standard, the residuals for both the velocity in the directions of X, Y and Z and the continuity must reach $10^{-4}$ and the energy residual reaches $10^{-6}$. However, the concentration of the pollutants is of primary concern. Hence, it is essential to ensure the residuals for $CO_2$ and CO reach $10^{-4}$ too. The convergence of the data solution depends on the maximum allowable residual error which was set earlier. For instance, the concentration of the pollutants is said to be converging when the difference between the current and subsequent data is less than $1 \times 10^{-4}$. When every residual has converged according to their maximum allowable error, the calculation is completed. However, to ensure that the calculation indeed converged, hybrid initialization was activated.

### 2.5 Effects of Ventilation Modes

Two cases with different ventilation modes are listed in Table 4. For Case 1, it was examined under the condition in which the range hood was switched OFF and that all windows were opened. For Case 2, all windows were opened, and the range hood was turned ON.

**Table 4:** Cases with different ventilation modes

| Case | Ventilation mode |
|---|---|
| Case 1 | All windows opened; Range hood is turned off |
| Case 2 | All windows opened; Range hood is turned on |

Case 2 was the baseline model and was tested during the GIT. The same configuration of meshing was used for all models. The average concentrations of $CO_2$ and CO for both cases along the cooking area and the adjacent room were taken along Lines 2 and 3 as shown in Figure 3. The boundary conditions of the range hood are summarized in Table 5.

**Table 5:** Boundary conditions

| Location | Boundary condition | |
|---|---|---|
| | Case 1 | Case 2 |
| Range hood | Outlet velocity = 0 m/s | Outlet velocity = 1.88 m/s |

Apart from the outlet velocity of the range hood, all the prescribed boundary conditions were set the same as the baseline model. Comparison between Cases 1 and 2 was performed to examine the significant effects of using the range hood on $CO_2$ and CO concentrations. An additional case (Case 3) was also examined to determine the impact of outlet airflow velocity of the range hood on the level of pollutants. As shown in Table 6, all the prescribed boundary conditions for Cases 2 to 3 are the same except for the range hood velocity.

**Table 6:** Cases with different range hood velocity

| Case | Range hood velocity (m/s) |
|---|---|
| Case 2 | 1.88 |
| Case 3 | 5.22 |

## 3.0 RESULTS AND DISCUSSION

### 3.1 Effect of Different Ventilation Mode

The pollutants are expected to flow from the gas stove to the kitchen area and adjacent room. As a consequence, the concentration of $CO_2$ in both regions has increased. Figure 4 shows the mass fraction contour of $CO_2$ for Case 1. It can be observed that the closer to the pollutant source which is the gas stove, the higher the concentration of $CO_2$. There is a relatively lower concentration of $CO_2$ in the adjacent room. The contour is observed at 1.5 m plane above the floor, also known as the breathing zone is the primary concern. Case 1 represents a condition where both windows were opened, and the range hood was switched off.

Figure 5 shows the mass fraction contour of $CO_2$ for Case 2, where the range hood is switched on. It is very obvious that the concentration of $CO_2$ in the adjacent room has decreased significantly. When compared to Case 1 there is no orange colored zone appears and only bluish green colored region covers the cooking area and also the adjacent room as depicted in the figure. From those contours, it is evident that Case 2 has better ventilation mode since it shows a low concentration of $CO_2$ with a percentage of improvement of 78.8% when compared with Case 1. By allowing both windows to open, the concentration of $CO_2$ in the adjacent room is also improved by 84.5%.

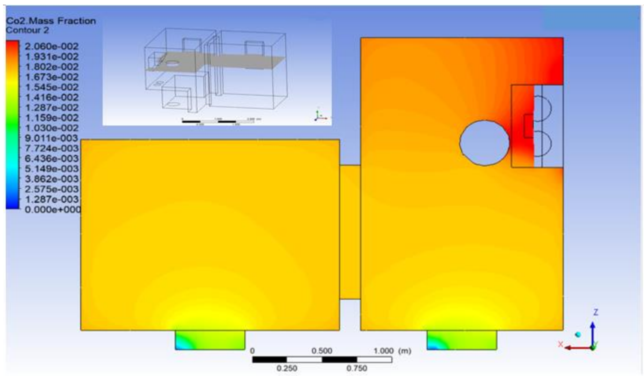


**Figure 4:** Distribution of $CO_2$ mass fraction for Case 1 (top view)


**Figure 5:** Distribution of $CO_2$ mass fraction for Case 2 (top view)

### 3.2 Effects of Range Hood Supply Ventilator

On average, the concentration levels for CO and $CO_2$ is collected along the cooking area and adjacent room for Cases 2 and 3. The data for $CO_2$ and CO for the two cases was then tabulated in Tables 7 and 8, respectively. For both cases, windows are widely opened. The improvement of reducing pollutants has been made by varying the range hood's velocity. Both tables prove that with a higher velocity of the range hood, the concentration of pollutants, $CO_2$ and CO could be decreased in both the cooking area and adjacent room. By comparing between Cases 2 and 3, the $CO_2$ gas concentration was reduced by 17.1% in the cooking area while the $CO_2$ level improved by 13.9% in the adjacent room. The CO gas level was reduced by 4.6% and 8.84% in the cooking area and adjacent room, respectively. Hence the concentration of $CO_2$ and CO gases could be improved in both spaces if the range hood is at a higher supply air velocity and the windows are widely opened.

**Table 7:** Average concentration of $CO_2$ in the cooking area and adjacent room

| Range hood velocity(m/s) | Average concentration $CO_2$ in cooking area (%) | Average concentration $CO_2$ in adjacent room (%) |
|---|---|---|
| 1.88 | 0.866 | 0.757 |
| 5.22 | 0.718 | 0.652 |

**Table 8:** Average concentration of CO in cooking area and adjacent room

| Range hood velocity(m/s) | Average concentration CO in the cooking area (%) | Average concentration CO in the adjacent room (%) |
|---|---|---|
| 1.88 | 0.461 | 0.452 |
| 5.22 | 0.440 | 0.412 |

## 4.0 CONCLUSION

A CFD model of a residential kitchen furnished with a single gas stove and a range hood was successfully developed and validated. The SST-$k\omega$ was selected as the flow model of the residential kitchen area. By installation of the range hood with a velocity of 1.88 m/s, the concentration of $CO_2$ is reduced to 0.866%. By changing the velocity of the range hood from the lowest to the highest speed, the average level of CO in the cooking area reduced by 4.56%, and 8.84% in the adjacent room. We can also conclude that the velocity of range hood is the most significant parameter for improving the contaminants level, i.e., by 17.09% when compared between the worst and best cases while the other conditions remain unchanged.

## ACKNOWLEDGMENTS

The authors acknowledge the Universiti Teknologi Malaysia (UTM) for providing the related facilities and technical support.

## NOMENCLATURE

| | | |
|---|---|---|
| CFD | | Computational Fluid Dynamics |
| CO | - | Carbon Monoxide |
| $CO_2$ | - | Carbon Dioxide |
| *drag F* | | Drag Force |
| $F_x$ | - | Additional Force |
| GIT | - | Grid Independent Test |
| $h$ | - | Enthalpy |
| $k$ | - | Molecular Conductivity |
| $k_t$ | - | Conductivity due to Turbulent Transport |
| NMRSE | - | Normalized Root Mean Square Errors |
| PAH | | Poly-Aromatic Hydrocarbon |
| $\rho$ | - | Static Pressure |
| $\rho g$ | - | Gravitational Body Force |
| $\rho_p$ | - | Particle's Density |
| RANS | | Reynolds Averaged *Navier-Stokes* |
| RNG | | Re-Normalization Group |
| $S_h$ | - | Volumetric Heat Source |
| SBS | | Sick Body Syndrome |
| SST | | Shear Stress Transport |
| T | - | Stress Tensor |
| UDF | | User Define Function |
| UFP | - | Ultra-Fine Particles |
| $v$ | - | Flow Velocity Vector Field |

## REFERENCES

1. Livchak A., Schrock D. and Sun Z., 2005. The Effect of Supply Air Systems on Kitchen Thermal Environment 2005, *ASHRAE Transactions*, 111(Part 1): 748-754.
2. Lim K. and Lee C., 2008. A Numerical Study on The Characteristics of Flow Field, Temperature and Concentration Distribution According to Changing The Shape of Separation Plate of Kitchen Hood System, *Energy and Buildings*, 40(2): 175-184.
3. ASHRAE Handbook 2004: HVAC Systems and Equipment, page 17.9

4. Yu K.P., Yang K.R., Chen Y.C., Gong J.Y., Chen Y.P. and Shih H.C., 2015. Indoor Air Pollution from Gas Cooking in Five Taiwanese Families, *Building and Environment*, 93(Part 2): 258-266.
5. Zhang H., Wang F., Wang Y. and Wang H., 2017. CFD Simulation of Cooking Particle Distribution and Motion, *Procedia Engineering*, 205: 1800-1806.
6. Xu A., Li H., Feng G., 2017. Numerical Simulation Analysis of Temperature and Pollutant Concentration Diffusion in The Open Kitchen Cooking Area, *Procedia Engineering*, 205: 1165-1172.
7. Zhou B., Chen F., Dong Z. and Nielsen P.V., 2016. Study on Pollution Control in Residential Kitchen Based on The Push-pull Ventilation System, *Building and Environment*, 107: 99-112.
8. MOUHRD of the PRC, GB/T18049-2000, 2000. *Secondary Determination of The PMV and PPD Indices of Thermal Environment and Thermal Comfort Condition of Provision*, China Standards Press, Beijing.
9. Lian L.M., 2007. *Engineering Thermodynamics*, 5$^{th}$ Edition, China Architecture and Building Press, Beijing.
10. Duan R., Liu W., Xu L., Huang Y. and Shen X., 2015. Mesh Type and Number for the CFD Simulations of Air Distribution in an Aircraft Cabin, *Numerical Heat Transfer, Part B: Fundamentals, An International Journal of Computation and Methodology*, 67(6): 489-506.
11. Li A., Gao M. and Zhang W., 2017. Field Test and CFD Modeling for Flow Characteristics in Central Cooking Exhaust Shaft of A High-rise Residential Building, *Energy and Buildings*, 147: 210-223.
12. Ferziger J.H., Peric M., 1999. *Computational Methods for Fluid Dynamics*, Berlin: Springer-Verlag.
13. Roache P.J., 1998. *Verification and Validation in Computational Science and Engineering*, Albuquerque, NM: Hermosa Publishers.